Organum vasculosum lamina terminalis-evoked postsynaptic responses in rat supraoptic neurones *in vitro*

Charles R. Yang, Vladimir V. Senatorov and Leo P. Renaud

Neurosciences Unit, Loeb Research Institute, Ottawa Civic Hospital and University of Ottawa, 1053 Carling Avenue, Ottawa, Ontario, Canada K1Y 4E9

1. To characterize the organum vasculosum lamina terminalis (OVLT) innervation of hypothalamic supraoptic nucleus (SON) neurones, current clamp recordings were obtained in SON cells in superfused rat hypothalamic explants. Stimulation of 1 Hz evoked 5–10 mV bicuculline-sensitive IPSPs in forty out of forty-six SON neurones, including both phasic (vasopressin immunoreactive) and continuously firing (oxytocin immunoreactive) cells.

2. In twenty-four cells, mean IPSP latency was 8·7 ± 1 ms (± S.D.) and reversal potentials (V_r) ranged between −60 and −75 mV. In the other sixteen cells, V_r ranged between −20 and −55 mV and the addition of bicuculline revealed underlying EPSPs (latency, 7·8 ± 0·8 ms; mean V_r, −8 ± 10 mV) with two components: (a) fast (rise and half-decay times of 5·83 ± 1·3 ms and 19 ± 4·4 ms respectively), with reversible blockade by 6-cyano-7-nitroquinoxaline-2,3-dione (CNQX); (b) slow (4- to 5-fold increase in rise and half-decay time), with reversible reduction by (−)-aminophosphonovaleric acid (APV).

3. During 10 Hz stimulation, EPSPs summated into 3–7 mV depolarizing envelopes lasting 1·5–3·0 s and sustaining action potential bursts. Depolarizing envelopes displayed voltage dependence, and were enhanced after removal of extracellular magnesium, diminished by APV and completely abolished by APV and CNQX together.

4. Thus, non-NMDA receptors probably mediate fast EPSPs whereas NMDA receptors mediate slow EPSPs and depolarizing envelopes. OVLT-evoked EPSPs were only seen in vasopressin-immunoreactive neurones.

5. These observations indicate converging inhibitory and target-selective excitatory amino acid-mediated inputs from OVLT to SON; the latter may modulate the excitability of SON vasopressin neurones to a hyperosmotic challenge.

The pioneering experiments of Jewell & Verney (1957) clearly indicated that the area of the hypothalamic supraoptic nucleus (SON) was a key structure in central nervous system (CNS) control of neurohypophysial hormone release consequent to a hyperosmotic challenge. Additional importance for CNS regulation of body fluid homeostasis has been placed on an area designated as the anterior ventral third ventricle (AV3V), and more specific structures located along the lamina terminalis (reviewed in Johnson, 1985; McKinley, McAllen, Mendelsohn, Allen, Chai & Oldfield, 1990). The AV3V incorporates a ventral portion of the lamina terminalis which is composed of three interconnected groups of neurones: the subfornical organ (SFO) which is located dorsally, the nucleus medianus (NM) surrounding the anterior commissure, and the organum vasculosum lamina terminalis (OVLT) positioned ventrally (see McKinley *et al.* 1990). Following electrolytic lesions in the AV3V that encompass the OVLT, animals subjected to a hypertonic challenge exhibit a selective attenuation of drinking and of vasopressin and oxytocin release, a persistent hypernatraemia and a blunted natriuresis (Thrasher, Keil & Ramsay, 1982; Johnson, 1985; McKinley *et al.* 1987; Leng, Blackburn, Dyball & Russell, 1989). SON neurones demonstrate an intrinsic osmosensitivity (Bourque, 1989), and receive afferents from neurones located in each of the cell groups along the lamina terminalis (Phillips & Camacho, 1987; Wilkin, Mitchell, Ganten & Johnson, 1989). Although the functional nature of these pathways remains undefined, the observation that lamina terminalis neurones also have an apparent osmosensitivity (Sibbald, Hubbard & Sirrett, 1988; McAllen, Pennington & McKinley, 1990; Vivas, Chiaraviglio & Carrer, 1990; Nissen, Bourque & Renaud, 1993) suggests that cells in all of these areas act in concert with the magnocellular neurosecretory neurones as

components of a central osmoreceptor complex to maintain hydromineral homeostasis (Dyball & Leng, 1989; Honda, Negoro, Dyball, Higuchi & Takano, 1990).

In the present study we used intracellular current clamp recordings from rat SON neurones in hypothalamic explants and defined the nature and pharmacology of their postsynaptic responses to electrical stimulation in OVLT. We now report that OVLT stimulation evokes $GABA_A$ receptor-mediated inhibitory postsynaptic potentials (IPSPs) in most SON neurones, whereas the same stimulus evokes glutamate NMDA and non-NMDA receptor-mediated excitatory postsynaptic potentials (EPSPs) that are selective for vasopressin-secreting neurones. A preliminary account of these results has been reported previously (Yang & Renaud, 1991; Yang, Senatorov & Renaud, 1992).

METHODS

Preparation

Experiments were performed on hypothalamic explants obtained from adult (180–220 g) male Long–Evans rats. Following acute decapitation the brain was removed and a horizontal explant of basal forebrain containing the SON prepared and pinned onto a Sylgard base in a temperature-regulated (34 °C) chamber. The cerebral vessels and membranes overlying both the OVLT and the SON were quickly removed. Retraction and cutting of the optic nerves at the optic chiasma exposed the OVLT located in the optic recess. The areas overlying the SON and the OVLT were superfused by oxygenated (95 % O_2, 5 % CO_2) standard artificial cerebral spinal fluid (ACSF), delivered by gravity at 0·9–1·3 ml min^{-1} and flowing from the SON area towards the OVLT. Standard ACSF (pH 7·4) comprised (mM): NaCl, 126; KCl, 3; $MgCl_2$, 1·3; $NaHCO_3$, 25·9; $CaCl_2$, 2·4; glucose, 10; and had an osmolality of 290–295 mosmol (kg water)$^{-1}$ as determined by freezing-point osmometry. Modifications of the ACSF used for different experiments are specified in the text. The level of ACSF and the direction of its flow were adjusted with cotton wicks to mimimize the electrode capacitance. Recordings were commenced after 2 h to allow for equilibration.

Electrophysiology

Intracellular recordings were obtained through glass micropipettes filled with either potassium acetate (KAc, 3 M, pH 7·4), a mixture of potassium acetate and potassium chloride (3 M KAc + 0·1 M KCl), or 1·5 % biocytin in 1·5 M KAc, 0·25 M KCl, with 0·025 M Tris buffer (pH 7·2). The microelectrode was connected to the input headstage of an Axoclamp-2A amplifier (Axon Instruments, Foster City, CA, USA). Throughout all of the recording sessions, bridge balance

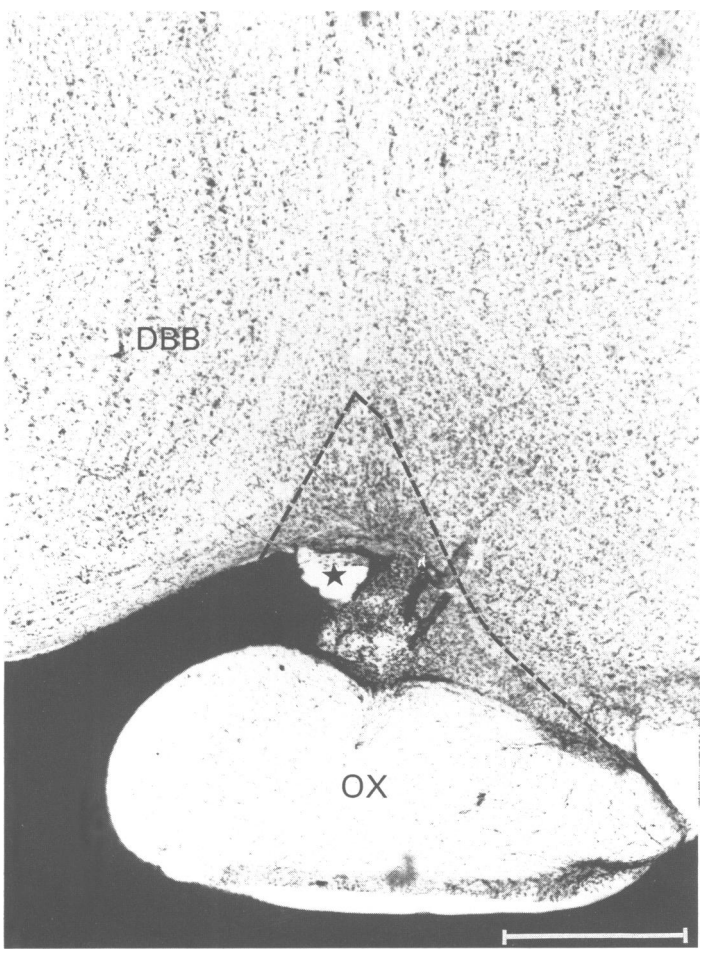

Figure 1. Stimulation site in OVLT
Cresyl Violet-stained photomicrograph of a coronal section through the basal forebrain at the level of the diagonal band of Broca (DBB). The filled star positioned dorsal to the optic chiasma (OX) indicates the site of a microlesion placed at the tip of the OVLT stimulation electrode. Calibration bar, 0·5 μm.

was maintained as a means of eliminating the time-independent component of the voltage response occurring at the onset and offset of rectangular current pulses that were applied through the recording electrode. Values for the resting membrane potentials were derived from the difference between the potential inside the cell and that when the electrode was withdrawn from the neurone at the end of the recording period. Input resistance was determined from the slope of voltage–current (V–I) plots obtained from membrane voltage deflections following delivery of a series of 100 ms depolarizing and hyperpolarizing current pulses. Changes in junctional potential at the indifferent electrode were minimized by connecting a Ag–AgCl reference electrode to the bath solution via a KCl–agar bridge. Amplified signals were digitized by a pulse-code modulator, sampled on-line using commercially available software (pCLAMP version 5.5.1, Axon Instruments) and recorded on videotapes for analysis off-line.

Electrical stimulation in OVLT was achieved through a stainless steel concentric bipolar stimulation electrode (SNE-100, Rhodes Medical Instruments, Woodland Hills, CA, USA) positioned at the ventral surface of the OVLT at the anteroventral mid-line wall of the third ventricle, dorsal to the optic chiasma (Fig. 1). In order to minimize activation of the adjacent tissue, e.g. the ventral portion of the nucleus medianus, the tip of the electrode was positioned only on the pial surface, without penetration. Monophasic square pulses (0·2 ms in duration, $\leqslant 300$ μA in intensity) were delivered at 1–10 Hz through a stimulation isolation unit. Peak amplitudes and the time to peak of EPSPs and IPSPs were measured from onset; half-decay times were measured from peak. Group data were expressed as means ± S.D. and comparisons were made using Student's t test.

Pharmacology

Antagonists applied in order to test for an effect on post-synaptic events included the following: mecamylamine and hexamethonium hydrochloride (10–50 μM) for nicotinic acetylcholine receptors; kynurenic acid (500–800 μM), for excitatory amino receptors; (−)-aminophosphonovaleric acid (APV; 20–50 μM) for NMDA receptors; 6-cyano-7-nitroquinoxaline-2,3-dione (CNQX; 10–20 μM) for non-NMDA receptors; bicuculline methiodide (BICC, 10–25 μM) for $GABA_A$ receptors; 2-hydroxy-saclofen (20–100 μM) for $GABA_B$ receptors; Losartan (DuP753, 1–5 μM) for angiotensin-II AT_1 receptors; proglumide (50 μM) for cholecystokinin receptors. All agents were bath applied, and all (except DuP753, a gift from Du Pont, NJ, USA) were purchased from Research Biochemicals Inc., MA, USA.

Histology and immunohistochemical identification

After each recording session the OVLT stimulation site was marked by passing a 10 μA DC current through the stimulation electrode. Explants were fixed in 4% paraformaldehyde in 0·1 M phosphate buffer for at least 24 h, reimmersed in phosphate buffer containing 20% sucrose (w/v), then sectioned on a vibratome or cryostat and stained with Cresyl Violet for histological examination (Fig. 1).

The technique used for immunohistochemical identification of the recorded neurones was modified from published protocols (Erickson, Ronnekleiv & Kelly, 1993). Briefly, adjacent, alternative SON sections were washed in 0·05 M Tris saline (3 times, 10 min each) and incubated with mouse monoclonal antibodies against either vasopressin (1:200 dilution) or oxytocin (1:150 dilution). The sections were then washed in 0·05 M Tris saline (3 times, 10 min each) and incubated in a mixture of horse-anti-mouse antibodies conjugated with fluorescein isothiocyanate (FITC, 1:100 dilution) and avidin conjugated with Texas Red (1:250 dilution) for 1–2 h at room temperature. The primary antibodies (gifts from Dr A. J. Silverman, Columbia University, NY, USA), and the mixture of secondary antibodies–FITC and avidin–Texas Red (both from Vector Laboratory, MO, USA), were diluted in 0·7% seaweed gelatin (Lambda Carrageenan, Sigma, USA), 0·5% Triton X, 3% bovine serum albumin in 0·05 M Tris saline. To minimize background staining, 1% normal horse serum was added to the Tris saline used for washing in some experiments. Following rinsing in Tris saline, sections were mounted on microscope slides and coverslipped with glycerol–phosphate buffer saline mixture (3:1 v/v) containing 2% N-propylgallate (Sigma) to prevent photo-bleaching. The sections were then scanned under a fluorescence microscope (Axiophot, Zeiss) for either vasopressin- or oxytocin-positive neurones (excitation filter bandpass 450–490 nm for FITC) which were also double-labelled with biocytin (excitation filter bandpass 532–560 nm for Texas Red). For black and white photographs, Kodak TMAX-400 film was used.

RESULTS

Data were obtained from a total of ninety-five SON neurones with resting membrane potentials ranging between −55 and −63 mV, input resistances of 75–300 MΩ and action potentials exceeding 70 mV. A smaller number of neurones were used for detailed analyses. Stable recordings lasting for 1–4·5 h permitted multiple drug tests and recoveries to be carried out in a select number of neurones, resulting in overlapping groups of responsive cells in certain tests. As noted in previous studies in SON neurones, spontaneous activity was characterized by either a phasic ($n = 26$) or a continuous ($n = 10$) firing pattern (reviewed in Renaud & Bourque, 1991). All SON cells demonstrated two additional features deemed to be typical of recordings from neurosecretory neurones, i.e. activity-dependent spike broadening, and the presence of an 'A'-notch as a result of an activation of a transient outward K^+ current when the cell was depolarized from holding potentials more negative than −70 mV (see Renaud & Bourque, 1991).

OVLT-evoked IPSPs

In forty of forty-five (89%) neurones recorded during perfusion with standard ACSF, electrical stimulation of the OVLT area evoked prominent 5–10 mV IPSPs at a latency of 8·7 ± 1 ms. At resting potentials, these evoked IPSPs had a mean rise time (to peak) of 5·76 ± 1·2 ms and a half-decay time of 10·24 ± 3·7 ms (measured from peak). Spontaneous activity in both phasically and continuously firing cells was interrupted transiently during these IPSPs (Fig. 2).

For these forty neurones, OVLT stimulation applied during steady-state membrane voltage deflections revealed reversal potentials (V_r) over a wide range, i.e. −20 to −75 mV. However, data selection indicated twenty-four cells with a more consistent V_r range of −60 to −75 mV (mean, −69 ± 5·6 mV) that approximated the equilibrium potential for chloride ions. In these instances, bath

application of BICC, but not 2-hydroxy-saclofen (only 8 cells were tested), completely and reversibly blocked these IPSPs (Fig. 2). At these concentrations, BICC did not result in any change in baseline membrane potential or input resistance.

OVLT-evoked EPSPs

Single-pulse stimulation

In sixteen of forty neurones in which OVLT-evoked responses appeared to be more complex, and V_r was in a more positive range, bath application of BICC to block any IPSP component revealed the presence of EPSPs, some of which triggered spike discharges (Fig. 3). This manoeuvre produced a further positive shift of their mean V_r from $-53{\cdot}4 \pm 5{\cdot}4$ to -8 ± 10 mV (Fig. 4). The latencies of evoked EPSPs ($7{\cdot}8 \pm 0{\cdot}8$ ms) were similar to those of evoked IPSPs. EPSP amplitudes ranged from 4 to 7 mV and demonstrated graded increases in amplitude as the stimulation intensity was progressively increased (Fig. 5*A*).

In seven of eight neurones that displayed spontaneous phasic firing, a pattern considered to be typical of most vasopressin-synthesizing neurones (Renaud & Bourque, 1991), delivery of a single OVLT stimulus, when the cells were current clamped just below threshold for firing (-62 to -55 mV and in the presence of BICC), elicited a short train of action potentials ($n = 7$). The length of the burst could be prolonged by either an increase in stimulation intensity or by further membrane depolarization (Fig. 5*B*).

EPSPs evoked in ACSF containing BICC possessed two distinct components. When cells were held at hyperpolarized potentials (-70 to -80 mV), OVLT-evoked responses consisted of *fast* EPSPs with a mean rise time of $5{\cdot}83 \pm 1{\cdot}3$ ms, a half-decay time of $19 \pm 4{\cdot}4$ ms, and a peak amplitude that was voltage independent, exhibiting a progressive increase with increasingly negative holding potentials. In four cells tested, the mean EPSP amplitude was reduced to 14 ± 12 % of the control value in the presence of kynurenic acid, with no change in membrane potential or input resistance. In ten other cells tested, the mean EPSP amplitude was also reduced to 33 ± 7 % of the control value in the presence of CNQX (Fig. 6). While five of these cells demonstrated that application of CNQX alone hyperpolarized the cell membrane by 2–3 mV, the antagonist actions of CNQX persisted when membrane

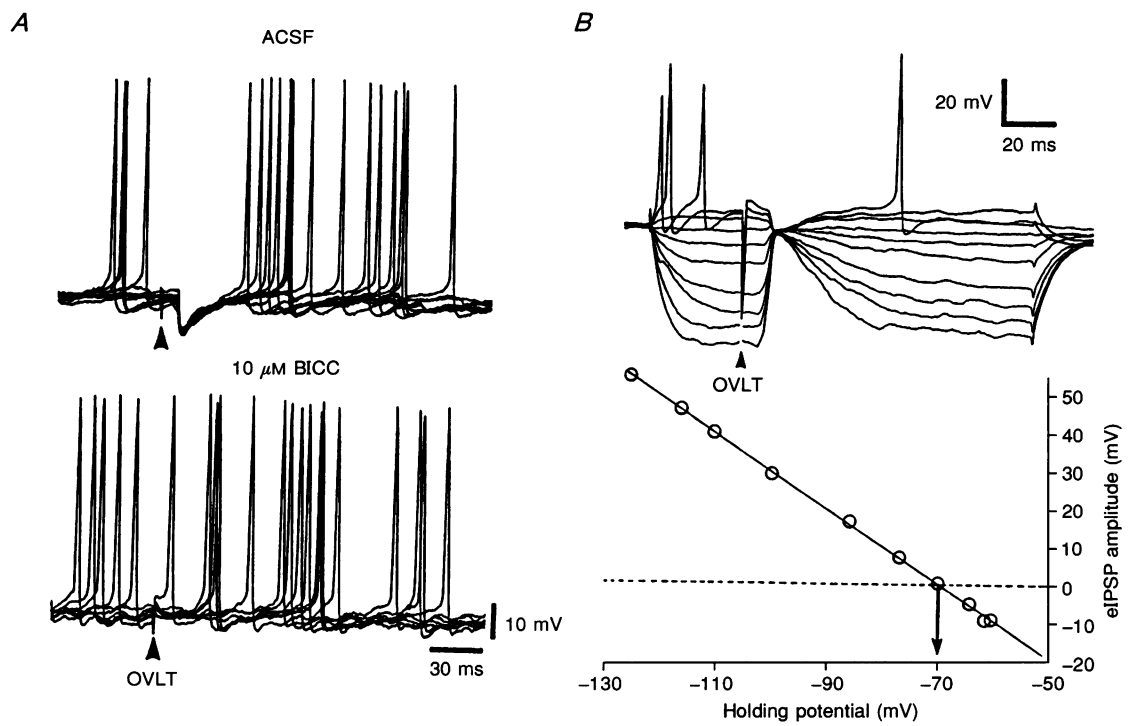

Figure 2. Features of OVLT-evoked IPSPs

A, superimposed voltage traces in the upper panel recorded from a spontaneously active SON neurone in control ACSF reveal that OVLT stimulation (arrowhead, 1 Hz) is followed by a short latency IPSP which transiently interrupts on-going activity. In the presence of bath-applied bicuculline (BICC, lower panel), OVLT-evoked IPSPs in the same neurone are blocked. *B*, the upper panel displays a progressive reversal of an OVLT-evoked IPSP from another SON neurone as membrane voltage is moved to more hyperpolarized ranges during 200 ms current pulse injections. A plot of the net change in PSP amplitudes (i.e. evoked potential, eIPSP: holding potential − IPSP amplitude) against the holding potentials in the lower panel indicates a reversal potential (V_r) for the IPSP at -70 mV (arrow), corresponding to the equilibrium potential for Cl^- ions.

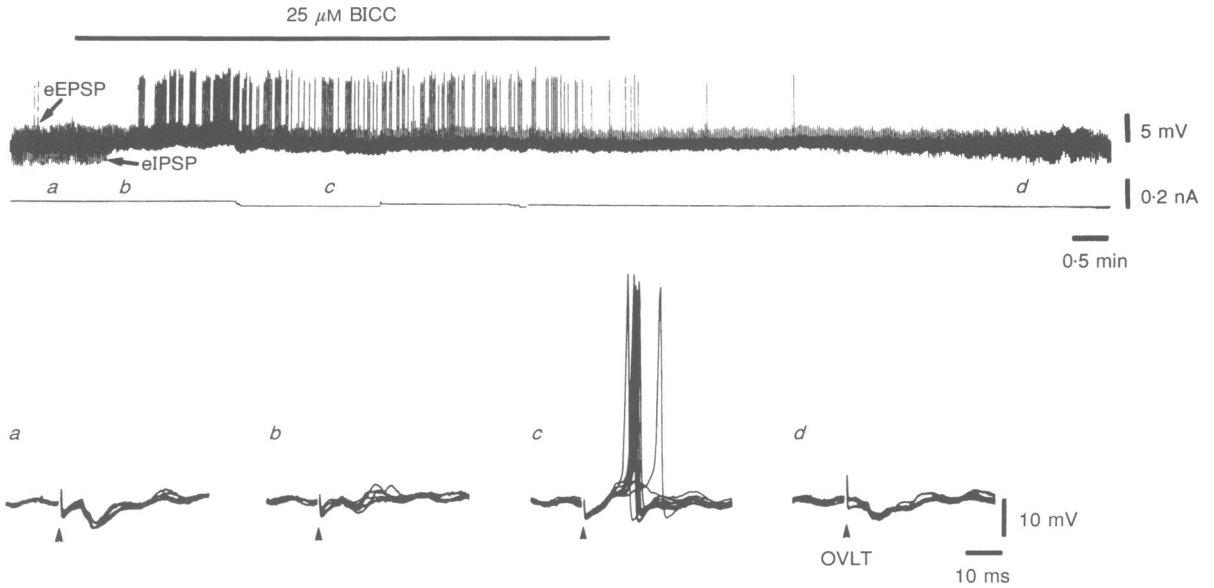

Figure 3. Bicuculline blocks IPSPs and reveals OVLT-evoked EPSPs
The upper panel is a continuous voltage record during application of single OVLT shocks at 1 Hz; the thin line below indicates continuous DC current injected to maintain a constant membrane voltage of −60 mV. Initially, each shock (in control ACSF) evokes both an EPSP (eEPSP), which occasionally triggers an action potential, and an IPSP (eIPSP); details are revealed in the expanded superimposed traces in the lower left panel (*a*; stimulus is applied at the arrowhead). With the addition of bicuculline (BICC; continuous line) to the perfusion media, eIPSPs are gradually blocked (*b*), leaving an eEPSP that frequently triggers action potentials (*c*). eIPSP blockade gradually recovers after return to control ACSF (*d*).

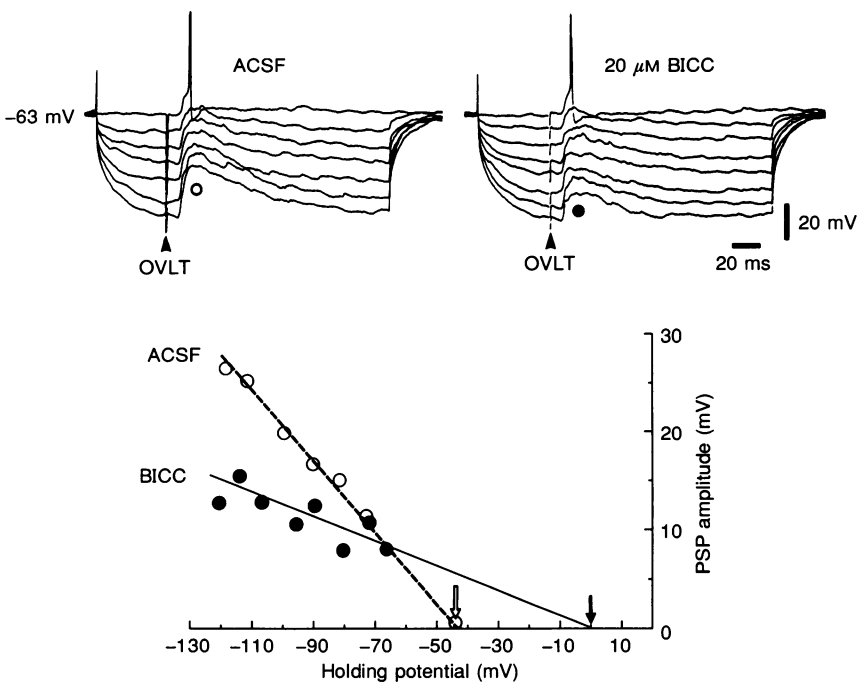

Figure 4. PSP reversal potential shifts after $GABA_A$ receptor blockade
In the upper left panel, records obtained in control ACSF reveal OVLT-evoked (at arrowhead) postsynaptic potentials at different holding potentials. Data shown are from 1 of 16 cells. In the upper right panel, a similar protocol for this cell obtained in the presence of bicuculline (BICC) reveals attenuation of the evoked PSPs. Below, a plot of the net PSP amplitude (measured at the open and filled circles) against the holding potential reveals a reversal potential shift from −45 mV (open arrow) to −4 mV (filled arrow). Lines were computed by regression analysis.

potential was clamped to the control level by intracellular current injection. Full recovery from CNQX required approximately 20 min.

Although reduced in amplitude, a component of the evoked responses generally persisted in CNQX, a feature that was particularly obvious when membrane potentials in the same cells were held at more depolarized levels ($\leqslant -65$ mV; see Fig. 6). The fact that NMDA receptor-mediated responses are known to be regulated by a voltage-sensitive Mg^{2+} block (see Mayer & Westbrook, 1987) suggested that this residual EPSP might represent an NMDA receptor-mediated component.

In order to characterize further this residual EPSP component, cells were retested in nominally Mg^{2+}-free ACSF (at least 30 min after initiating this procedure). Under these circumstances, OVLT stimulation was now seen to evoke *slow* EPSPs whose mean rise time was 30 ± 10 ms and mean half-decay time 165 ± 45 ms (Fig. 7*A* and *C*). Under such circumstances, as the membrane potentials were current clamped progressively at holding potentials between -55 and -120 mV, the peak amplitude of these EPSPs increased while their half-decay times were markedly reduced (Fig. 7*A* and *B*). Upon reintroduction of 1·2 mM Mg^{2+} to the ACSF, the effects were reversible, the most striking being the reduction in EPSP half-decay time across all holding potentials, except when membrane potentials were held at more positive values than -65 mV, at which point a trend towards an increase in half-decay times began to appear (Fig. 7*B*). The overall half-decay time of fast EPSPs evoked in standard ACSF was 4- to 5-fold shorter than the slow EPSPs evoked in zero $[Mg^{2+}]_o$.

In zero Mg^{2+} and bath-applied APV, the half-decay time of the OVLT-evoked EPSP was reduced to 38 ± 19 % of control ($P < 0{\cdot}001$; $n = 6$) whereas the peak amplitude remained at $89{\cdot}6 \pm 2$ % of control (Fig. 7*C*). Reintroduction of 1·2 mM Mg^{2+} in the continued presence of APV resulted in a reduction of *both* the peak EPSP amplitude (61 ± 12 %) *and* the half-decay time (30 ± 24 %) relative to values in

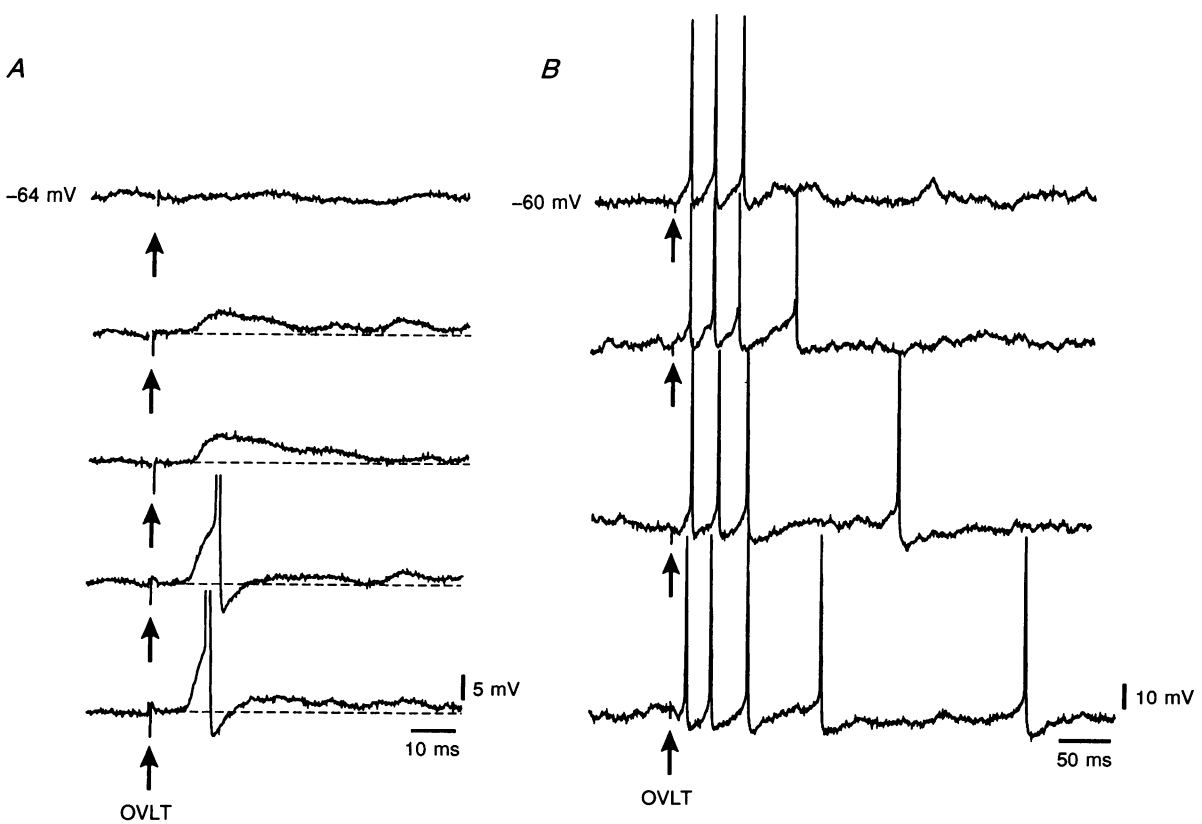

Figure 5. OVLT stimuli (1 Hz; arrows) evoke graded excitatory responses according to stimulus strength

A, note the change in EPSP shape and amplitude as the stimulus strength is increased from subthreshold (top trace) to 1·4 times threshold (lowest trace) in a SON neurone held at -64 mV. Action potentials (truncated) are evoked at the higher stimulation intensities. *B*, voltage traces from another cell where membrane potential is held closer to threshold (-61 mV). Note the progressive increase in response as the stimulation strength is increased from 1·3 times threshold (in the top trace) to 1·6 times threshold (in the bottom trace).

zero Mg^{2+} (Fig. 7C). At this point, further addition of CNQX virtually abolished any remaining EPSPs. Under all these pharmacological treatments, EPSP latencies remained constant.

Repetitive (10 Hz) stimulation

Additional features of interest in the OVLT-evoked responses were obtained using a 10 Hz, 1 s train of stimuli. In standard ACSF containing BICC, cells held at membrane potentials of $\leqslant -65$ mV displayed successive summation of EPSPs into a 3–7 mV *slow depolarizing envelope* that outlasted the stimulation period by 1·5–3 s, and generated several action potentials as threshold levels were reached. The time to peak for this slow depolarizing envelope was 0·67 ± 0·2 s, achieved with the 5th to 8th stimulus (Fig. 8).

As in the analyses with single evoked EPSPs, the introduction of selective glutamate receptor antagonists permitted detection of the contribution of both NMDA and non-NMDA glutamate receptor subtypes to these depolarizing envelopes. In APV, the slow depolarizing envelope was reduced to 6 ± 23 % of control, leaving individual fast EPSPs; in CNQX, fast EPSPs were reduced to 13 ± 20 % of control, without affecting the underlying slow depolarizing envelope (Fig. 8). It was also noted that CNQX in excess of 25 μM not only blocked the EPSPs, but also the slow depolarizing envelope. However, neither fast EPSPs nor the slow depolarizing envelopes were sensitive to the application of other receptor antagonists, including Losartan ($n = 5$ cells), proglumide ($n = 3$ cells), mecamylamine and hexamethonium ($n = 7$ cells).

Depolarizing stimuli that trigger action potentials in SON neurones are known to activate a postspike depolarizing after-potential (DAP) whose summation can give rise to a composite depolarizing envelope and bursting discharge (Andrew & Dudek, 1984; Bourque, 1986; Andrew, 1987). In order to define a distinction between the NMDA receptor-mediated slow depolarizing envelope and these DAPs, experiments were conducted with membrane potentials held at > -70 mV in a voltage range where the DAP conductance is known to be inactivated (Bourque, 1986), and in zero Mg^{2+} ACSF so as to maximize the NMDA receptor-mediated responses. Under these conditions, OVLT stimulation induced a pronounced enhancement of both the amplitudes of EPSPs and the slow depolarizing envelope when compared with the responses evoked in standard ACSF (Fig. 9). In APV, the slow depolarizing envelope was incompletely blocked (26 ± 12 % of control); addition of CNQX was needed to achieve complete (but reversible) blockade ($n = 5$ cells). The reduction in extracellular Mg^{2+} is presumed to lead to a reduction of membrane surface charge screening, thereby increasing Ca^{2+} conductance and consequently enhancing synaptic transmission (Hille, 1984). The APV-insensitive residual depolarization evoked by repetitive OVLT stimulation is most likely to be the result

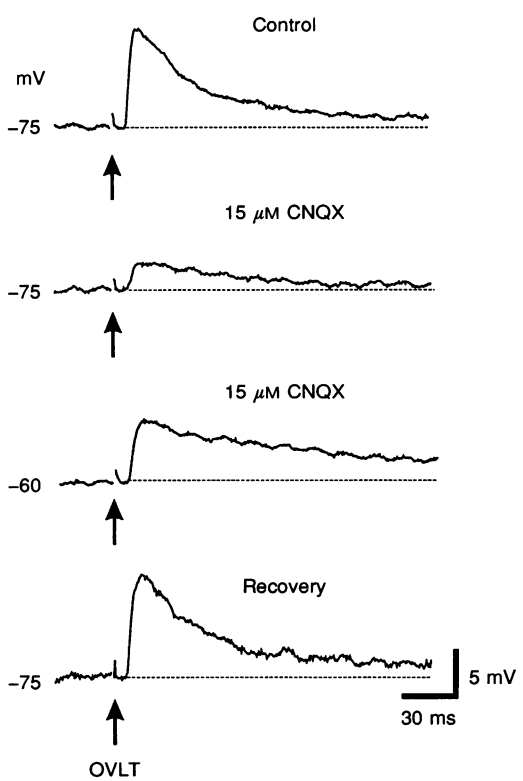

Figure 6. OVLT-evoked EPSPs recorded in the presence of bicuculline demonstrate two components
The upper trace recorded in ACSF containing 1·3 mM Mg^{2+} (Control) and at a holding potential of −75 mV displays a fast EPSP with a rise time of 10·4 ms and a half-decay time of 25 ms. After addition of CNQX to the media (second trace) there was a 90 % amplitude reduction, suggesting mediation via non-NMDA receptors. Note, however, that membrane depolarization to −60 mV (third trace) reveals a slow EPSP whose rise and half-decay times are prolonged. The lowest trace illustrates recovery 13 min after removal of CNQX.

of a summation of non-NMDA receptor-mediated EPSPs since further addition of CNQX abolished all residual depolarization.

Correlation of OVLT-evoked response with immunocytochemistry

Of the thirty-six neurones examined for their spontaneous firing activity, twenty-six cells demonstrated burst firing, with active periods that ranged widely between 400 ms and 162 s, and separated by silent intervals of 140 ms to 70 s. As illustrated in Figs 8 and 10, a 10 Hz OVLT stimulus consistently evoked a slow depolarizing envelope and burst firing. In five of these cells which initially exhibited continuous firing, membrane hyperpolarization through intracellular negative DC current injections transformed their continuous firing pattern to phasic firing. Eighteen of twenty-six neurones were labelled with biocytin in sufficient detail to reveal somata with fusiform or elongated shapes (approximate dimensions: $25 \times 12\ \mu m$) and two to three processes emerging from the soma. Successful double labelling in thirteen of the eighteen cells demonstrated vasopressin-like immunoreactivity (Fig. 10).

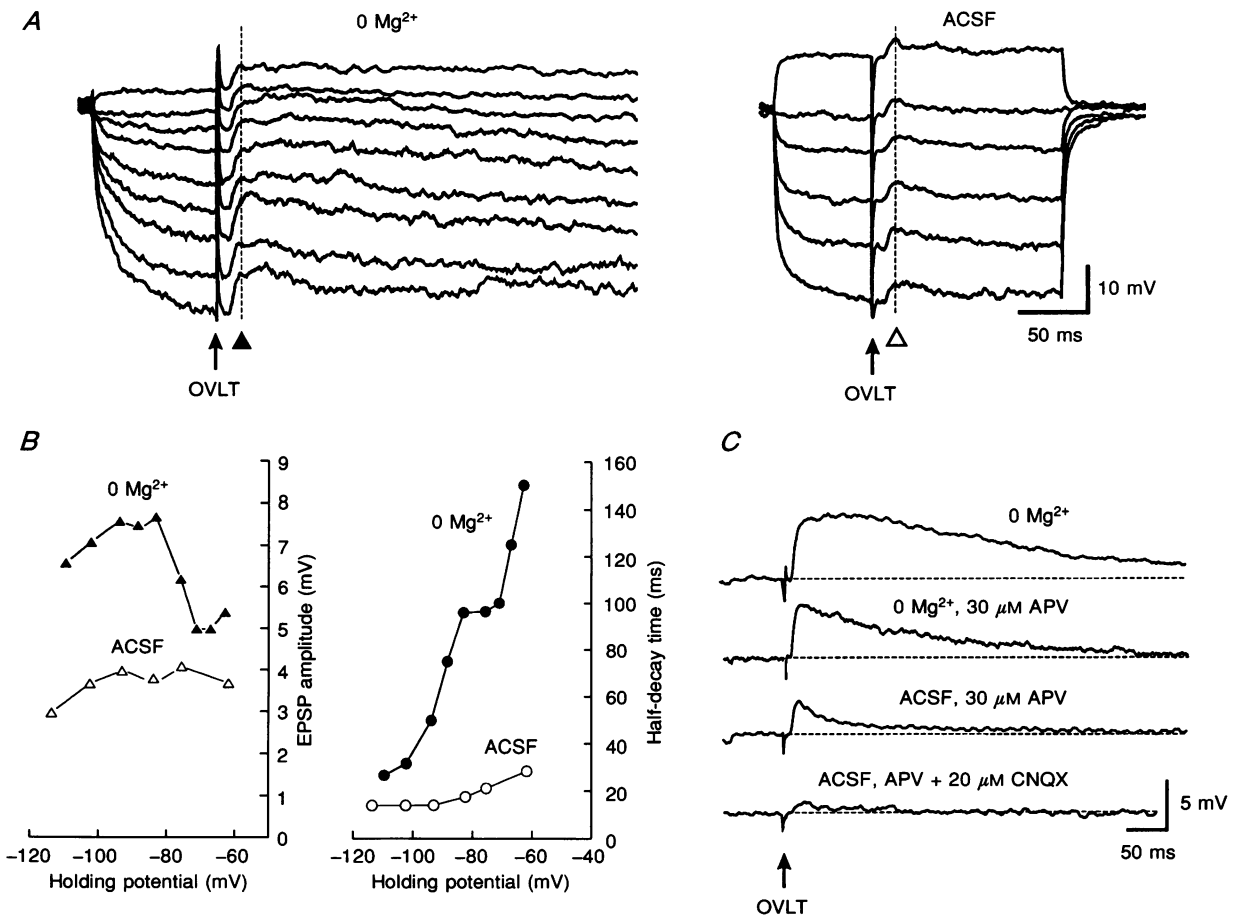

Figure 7. Holding potentials, extracellular Mg^{2+} and NMDA influence OVLT-evoked EPSPs
A, illustration of the different potentials observed from a SON neurone when records were obtained in nominally Mg^{2+}-free (0 Mg^{2+}) media (left panel) compared with standard ACSF (right panel). Note that as the holding potentials are current clamped to positive voltage ranges, EPSPs evoked by an OVLT stimulus (arrow) demonstrate a large increase of both peak amplitude and half-decay time when recorded in nominally Mg^{2+}-free media. *B*, plots of peak amplitudes (left) and half-decay times (right) obtained from the OVLT-evoked EPSPs recorded in standard ACSF and in nominally Mg^{2+}-free media under different holding potentials. Note that there is an overall increase in the peak amplitudes of the EPSPs recorded in Mg^{2+}-free media (▲) as compared to standard ACSF (△). There is also a 4- to 5-fold increase in EPSP amplitude when held at positive holding potentials in 0 Mg^{2+} (●) as compared to standard ACSF (○). *C*, voltage traces (each an average of ten responses) illustrating two components of 1 Hz OVLT-evoked EPSPs. In a neurone current clamped at −64 mV, EPSPs evoked in nominally Mg^{2+}-free media (top trace) have a long decay time. These EPSPs display reduced amplitude and duration in the presence of APV (second trace). Reintroduction of standard ACSF (containing 1·2 mM Mg^{2+} and APV) is associated with a marked reduction of both the amplitude and the half-decay time (third trace). The remaining fast EPSP is blocked in the presence of CNQX (lowest trace). All recordings were made in the presence of 15 μM bicuculline.

In contrast, ten continuously firing cells that displayed no apparent DAPs and whose activity could not be transformed into phasic or burst firing upon membrane hyperpolarization were completely unresponsive to repetitive OVLT stimulations; successful double labelling in six of these neurones revealed oxytocin-like immunoreactivity (Fig. 11).

DISCUSSION

Although projections from OVLT neurones to hypothalamic magnocellular neurosecretory neurones have been demostrated in several anatomical studies (McKinley *et al.* 1987; Phillips & Camacho, 1987; Wilkin *et al.* 1989), little information is available on the transmitters that may use such pathways, or their postsynaptic actions on SON neurones. The present observations support the involvement of amino acids in mediating inhibitory ($GABA_A$ receptors) and excitatory (glutamate NMDA and non-NMDA receptors) postsynaptic events as a prominent feature of the neuropharmacology of this OVLT–SON connection in the rat.

GABA-mediated IPSPs

In standard ACSF, OVLT-evoked responses in SON neurones are dominated by prominent compound IPSPs that we presume to be generated monosynaptically. Their selective sensitivity to BICC rather than to 2-hydroxysaclofen, and reversal potentials that approximate the equilibrium potential for chloride ions (≈ -70 mV) reflect the activation of $GABA_A$ receptors (Randle, Bourque & Renaud, 1986). This inhibition would also be a probable explanation for earlier *in vivo* observations where electrical stimulation of the AV3V region, of which OVLT is an integral part, was followed by a short latency, short duration reduction in the excitability of SON neurones

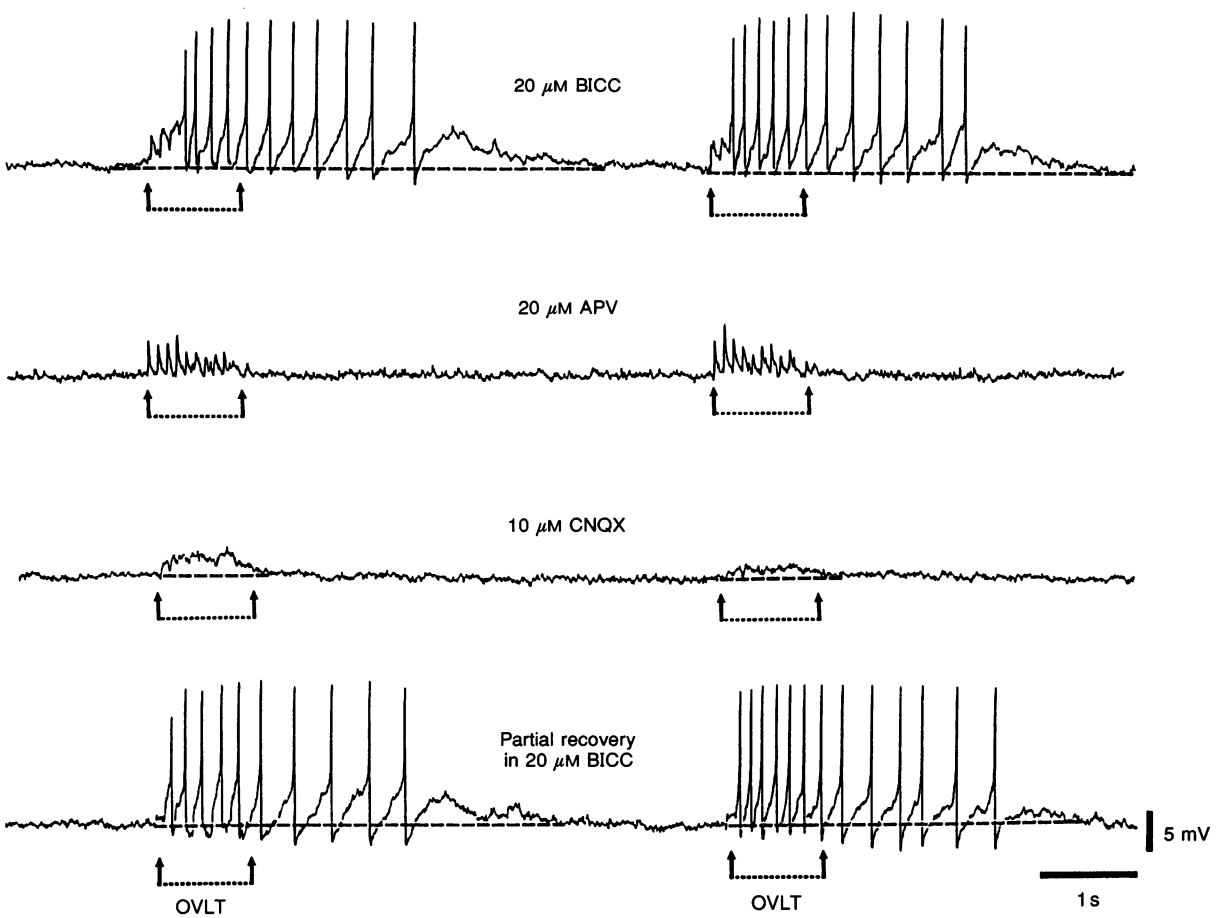

Figure 8. SON neurone response to 10 Hz OVLT stimuli
All recordings were obtained in the presence of bicuculline; OVLT stimuli were presented between the arrows. The top trace is a sequence of fast EPSPs that summate and give rise to a slow membrane depolarization (indicated above the dashed line) and burst of action potentials. In the presence of APV (second trace), individual fast EPSPs remain but the slow depolarization is abolished. In contrast, in the presence of CNQX (third trace), fast EPSPs are markedly reduced whereas the slow OVLT-evoked depolarizations persist. The lowest trace illustrates partial recovery. Membrane holding potential was -60 mV.

(Leng *et al.* 1989; Honda *et al.* 1990). The precise origin of this GABAergic innervation remains unclear. One possibility is that our results reflect the *en passage* activation of fibres originating from GABAergic neurones located in neural structures adjacent to the OVLT. Indeed, $GABA_A$-mediated IPSPs are readily observed in SON cells after electrical stimulation in the diagonal band of Broca (Jhamandas & Renaud, 1986; Randle *et al.* 1986), although anatomical studies would indicate that diagonal band efferents are not GABAergic, but rather project to a GABAergic interneurone (Jhamandas, Raby, Rogers, Buijs & Renaud, 1989). Another interesting possibility is that the GABAergic neurones themselves reside within the OVLT, a proposal that derives support from recent *in situ* hybridization data revealing the presence of mRNA for glutamic acid decarboxylase in neurones, along the entire lamina terminalis (OVLT included), that project to the magnocellular neurosecretory nuclei (Roland & Sawchenko, 1992).

Glutamate-mediated EPSPs

In the presence of BICC, the responses to OVLT stimulation are distinctly excitatory, indicating co-activation of

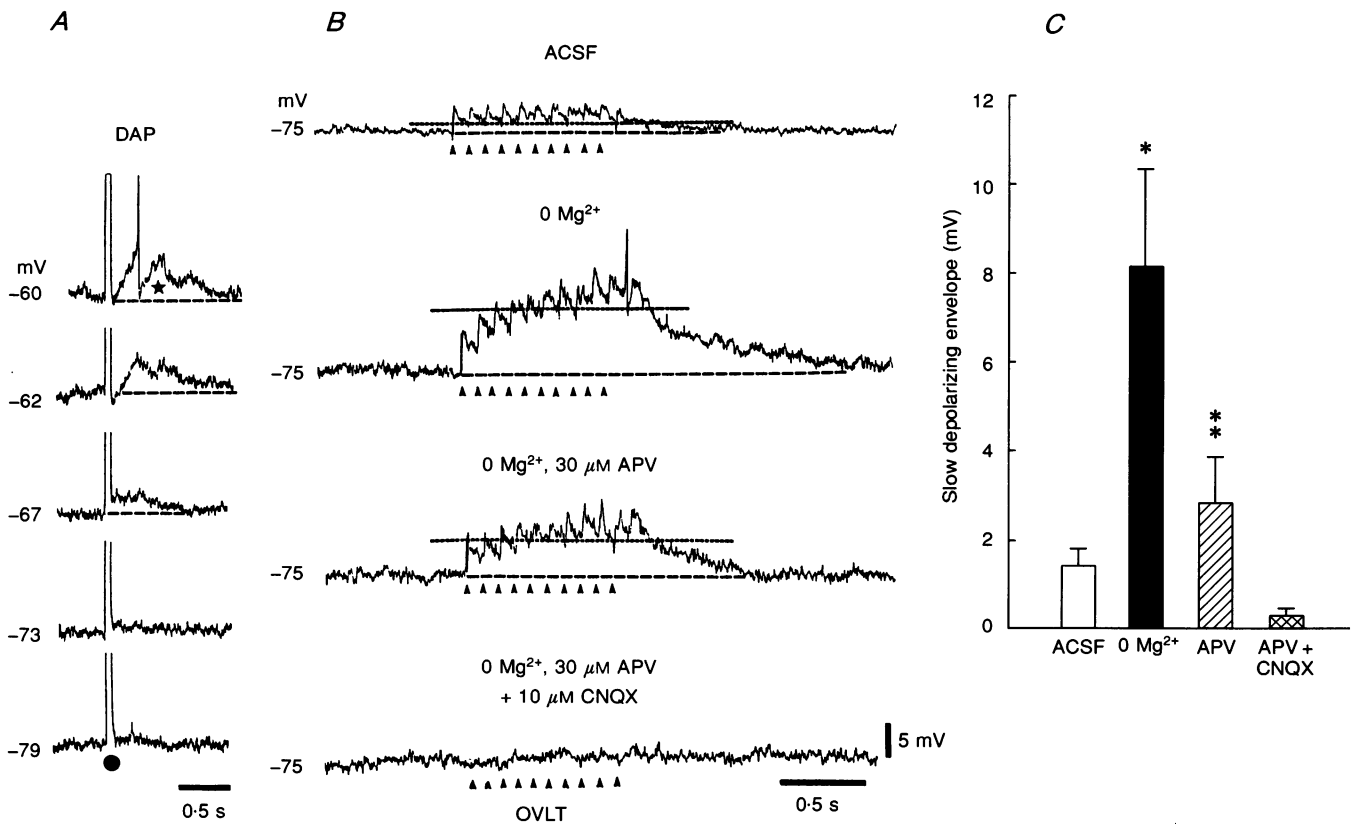

Figure 9. The intrinsic depolarizing after-potential (DAP) is dissociated from the OVLT-evoked slow depolarizing envelope

A, sequence of traces illustrating the voltage-dependent DAP (★) evoked by an intracellular depolarizing current pulse (●; 80 ms duration, 0·5 nA) sufficient to evoke 5 action potentials, recorded in standard ACSF. Since the DAP current is inactivated at membrane potentials beyond −70 mV (see Bourque, 1986), experiments were conducted in neurones held at > −70 mV in order to ensure that the OVLT stimulation did not simultaneously activate this conductance. *B*, traces recorded in standard ACSF containing bicuculline illustrate the effects of Mg^{2+} and glutamate receptor antagonists on fast EPSPs and the slow depolarizing envelope during a train of 10 Hz OVLT stimuli (arrowheads). The top trace shows the response in ACSF. Thirty minutes after switching from ACSF to nominally Mg^{2+}-free media, note the prominent increase in the slow depolarizing response (between the dotted line and the dashed line) and also a less marked increase in fast EPSP amplitude. In APV (third trace), the slow depolarizing potential is markedly reduced whereas all responses are virtually abolished with the further addition of CNQX (lowest trace). Stimulus artifacts were blanked for clarity. The dotted line marks the steady state on the plateau of the slow depolarizing envelope. *C*, data from 5 neurones are summarized in the histogram. Note the significant (*$P < 0{\cdot}001$) augmentation of the peak amplitude of the slow depolarizing envelope (■) in 0 Mg^{2+} when compared to ACSF (□), its significant (**$P < 0{\cdot}01$) attenuation in APV (▨) and further reduction when both APV and CNQX are present (▩). All data were obtained with the membrane potential held at −75 mV.

excitatory projections. These EPSPs are selectively sensitive to glutamate receptor antagonists, and components identified with both non-NMDA and NMDA receptor subtypes can be distinguished in the responses evoked by single and repetitive OVLT stimuli.

In response to a single stimulus, non-NMDA receptor-mediated EPSPs exhibit fast rise and decay times when held at membrane potentials more negative than rest ($\geqslant -65$ mV). NMDA receptor-mediated EPSPs feature slower rise and half-decay times when held more positive than rest ($\leqslant -65$ mV), and are significantly augmented in the absence of extracellular Mg^{2+}. The voltage range for the activation of the NMDA-mediated slow EPSPs falls within the negative slope conductance region (between -45 and -65 mV) determined from the current–voltage relationship of a typical NMDA-mediated response in SON cells (Hu & Bourque, 1991). In this depolarized voltage range, the normal voltage-dependent Mg^{2+} block would be relieved gradually, thus allowing full expression of the NMDA receptor-mediated mechanism (Mayer & Westbrook, 1987).

Within the response to a 10 Hz train of OVLT stimuli are two interesting features: a voltage-dependent slow depolarizing envelope containing superimposed fast EPSPs, and bursting discharges. The slow depolarizing envelope, which featured most prominently when activated in the membrane voltage range depolarized more than -65 mV and in the absence of extracellular Mg^{2+}, is reversibly blocked by NMDA receptor antagonist APV – all features that underly the synaptic activation of NMDA receptors (Herron, Lester, Coan & Collingridge, 1986; Collingridge, Herron & Lester, 1988). SON neurones contain both non-NMDA and NMDA receptors (Hu & Bourque, 1991) and the present observations indicate that both types of glutamate receptors can participate in a frequency- and voltage-dependent manner to modulate an OVLT-evoked postsynaptic response. We presume from these observations that the initiation of the slow depolarizing envelope requires summation of the non-NMDA receptor-mediated fast EPSPs in order to depolarize the membrane to a voltage range in which a voltage-dependent Mg^{2+} block of the NMDA receptor–channel complex can be relieved. At the frequency chosen (10 Hz), the prolonged decay time of the NMDA-mediated EPSPs would certainly facilitate successive summation of the repetitively evoked EPSPs (MacDermott & Dale, 1987) to induce the formation of a slow depolarizing envelope. The possibility of a co-ordinated mechanism between the two glutamate receptor subtypes is illustrated by the finding that high concentrations of CNQX not only blocked individual non-NMDA receptor-mediated EPSPs and prevented their summation to depolarize the membrane, but also blocked the induction of the NMDA receptor-mediated slow depolarizing envelope, presumably by competing with the glycine modulatory site of the NMDA receptor–channel complex (Lester, Quarum, Parker, Weber & Jahr, 1989).

Other transmitters

Angiotensin is another possible excitatory transmitter in the pathway from OVLT to SON, based on observations of angiotensin-like immunoreactivity in OVLT neurones labelled retrogradely following tracer injections in SON (Wilkin *et al.* 1989). Although SON neurones contain functional angiotensin AT_1 receptors whose activation produces membrane depolarization (Yang, Phillips & Renaud, 1992), bath-applied Losartan (a non-peptide AT_1 receptor antagonist), at concentrations that block angiotensin-evoked responses, had no apparent influence on OVLT-evoked excitation. This is in agreement with an earlier report (Leng *et al.* 1989) in which intracerebroventricular administration of the angiotensin peptide antagonist, saralasin, also had little influence on the firing of SON neurones evoked by A3V3 stimulation. Other studies in hypothalamic slice preparations reveal that a slow membrane depolarization can be evoked by single-pulse or high frequency stimulations delivered to the region situated dorsolateral to SON, and also its blockade by nicotinic and NMDA antagonists (Gribkoff & Dudek, 1990; Gribkoff, 1991). The possibility that the OVLT stimulations in this study activated a cholinergic input seems unlikely since bath application of the nicotinic receptor antagonists mecamylamine and hexamethonium failed to block the OVLT-evoked slow depolarization and bursting discharge.

OVLT inputs: selective to vasopressin-synthesizing neurones?

Our electrophysiological data reveal that OVLT stimulation activates phasically firing SON neurones selectively. Our immunohistochemical studies on biocytin-labelled SON neurones confirm that the activated neurones are immunoreactive to vasopressin rather than oxytocin. Somewhat different results were reported in lactating Wistar rats *in vivo* where oxytocin release followed intense (0·5 mA, 1 ms pulses), prolonged (15–25 s), high frequency (50 Hz) stimulation of the AV3V area (Blackburn, Leng & Russell, 1987). However, it is apparent that there are differences in stimulation sites; in the study by Blackburn *et al.* (1987), the most effective sites for the release of oxytocin were in or near the nucleus medianus and the diagonal band of Broca, sites that are dorsal to the OVLT and seemingly not involved in the present study.

Functional role(s) of OVLT–SON GABA and glutamate pathways

As components of a circumventricular organ, OVLT neurones are likely to be exposed to larger molecules present within the systemic circulation (Krisch, Leonhardt & Buchheim, 1978; McKinley *et al.* 1990). Thus, a variety of agents with receptors in OVLT may participate in the activation (or inhibition) of SON neurones. The OVLT is

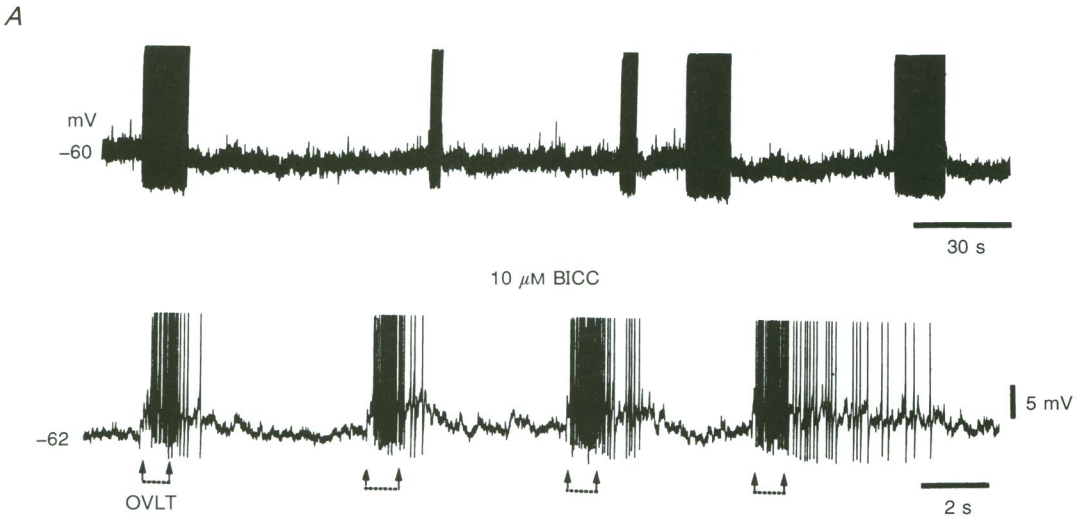

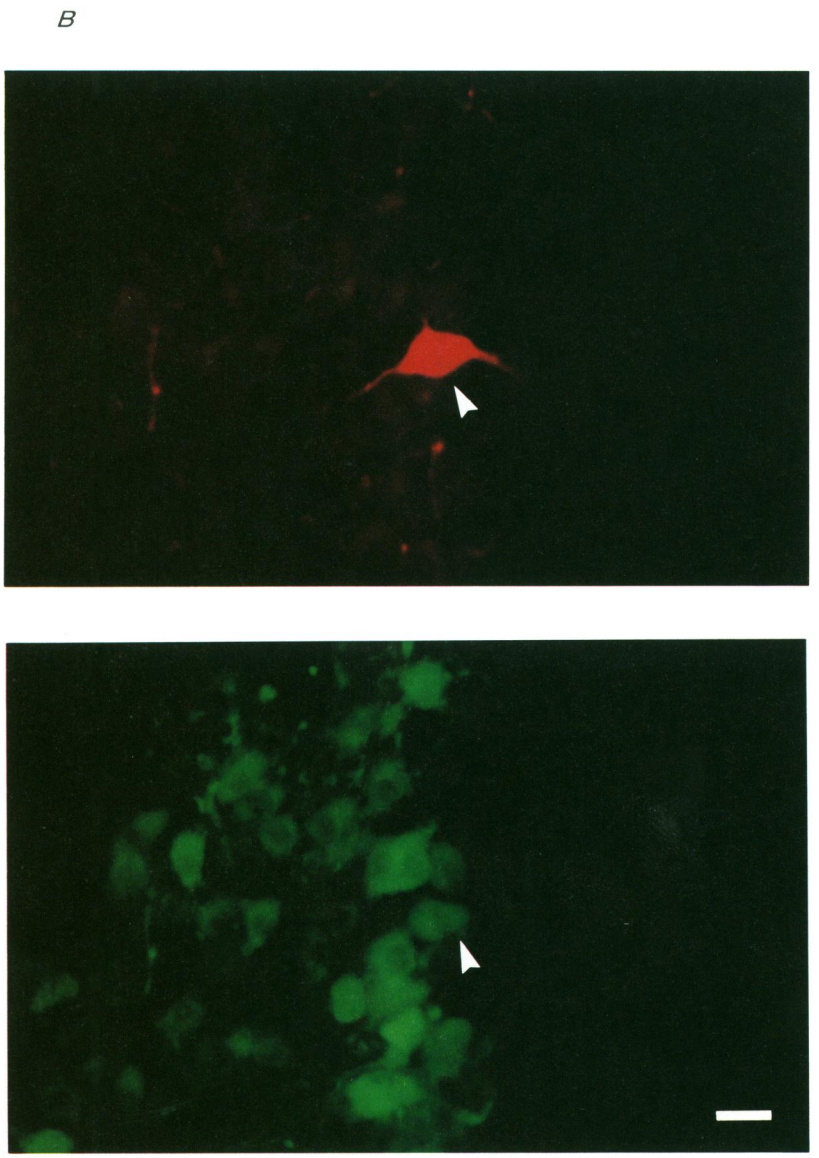

Figure 10. OVLT-evoked EPSPs are present in phasically active vasopressin-synthesizing SON neurones

A, the top panel displays a typical spontaneous phasic firing pattern in a SON neurone with variable active and interburst silent intervals when membrane potential is held at close to threshold (−60 mV). With this cell held at −62 mV, and in the presence of bicuculline, typical fast EPSPs and slow depolarization with an associated burst of action potentials (truncated) evoked during a 10 Hz train of OVLT stimulation are illustrated in the lower panel. *B*, the upper panel illustrates biocytin labelling of a neurone that exhibited the phasic firing pattern shown in *A*. The lower panel indicates that the same neurone (arrowhead) was among the cells that demonstrated vasopressin immunoreactivity. Calibration bar, 20 μm.

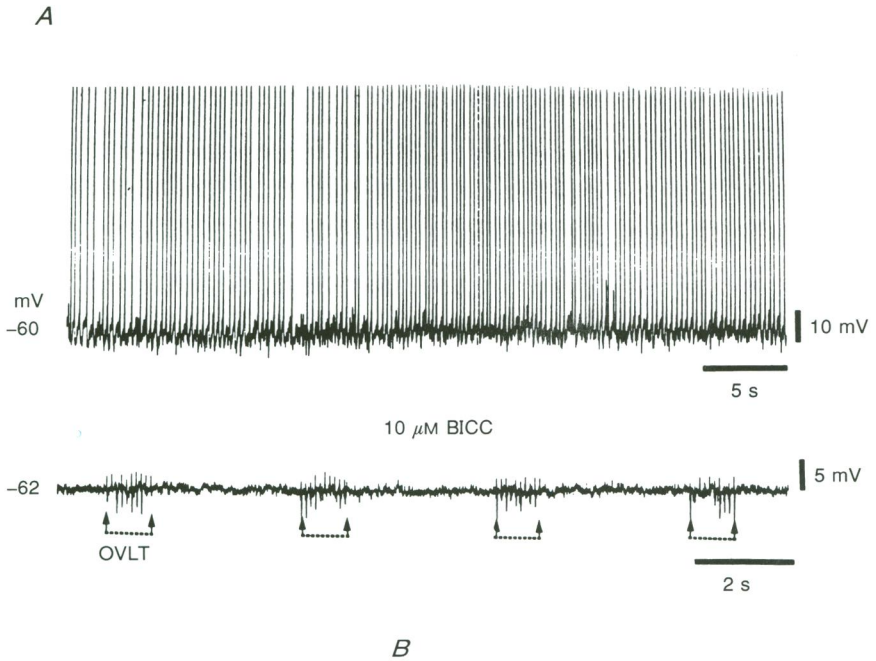

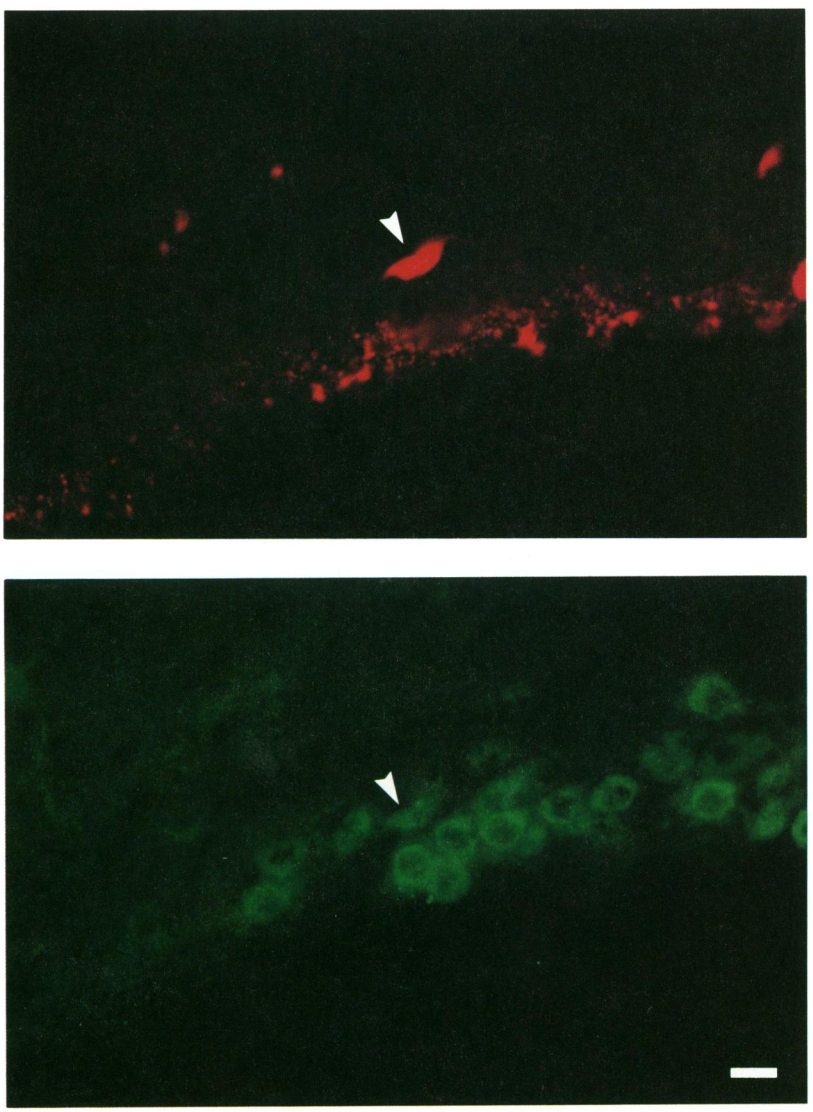

Figure 11. OVLT-evoked EPSPs are absent in continuously firing oxytocin-synthesizing SON neurones
A, the top trace demonstrates the continuous firing pattern in a SON neurone. Changing the membrane from −60 mV to more hyperpolarized levels did not change the pattern of activity to phasic firing, nor did this cell display a DAP (data not illustrated). The lower trace, obtained during a 10 Hz train of OVLT stimulation (intensity was supramaximal for evoking EPSPs in vasopressin-synthesizing cells), demonstrates the shock artifacts but no fast EPSPs or slow depolarizing envelope. The experiment was performed in the presence of 10 μM bicuculline. *B*, the upper panel illustrates biocytin labelling in a SON neurone that displayed continuous firing and showed no DAP. The lower panel indicates that this neurone (arrowhead) is among the oxytocin-immunoreactive cells in SON. Peptide immunoreactivity is cytoplasmic in location. Calibration bar, 20 μm.

unique among circumventricular organs by virtue of its participation in two important challenges that involve vasopressin: plasma hyperosmolality (Thrasher *et al.* 1982) and fever (Stitt, 1985). An appropriate homeostatic response to both of these stresses is likely to involve several neuronal cell groups. Osmoregulation involves an osmoreceptor 'complex' (Dyball & Leng, 1989). While the final output of this complex is at the level of the magnocellular vasopressin-secreting neurones possessing an intrinsic osmosensitive conductance (see Renaud & Bourque, 1991), their ability to respond can be enhanced by synaptic input from other neurones located along the lamina terminalis and AV3V area (Chaudhry *et al.* 1989; Honda *et al.* 1990). The OVLT is an AV3V structure that contains osmosensitive neurones (Vivas *et al.* 1990; Nissen *et al.* 1993). The *in vivo* application of osmotic stimuli in this area produces activation of SON neurones (Honda *et al.* 1990). Moreover, the application of hyperosmotic media to OVLT *in vitro* increases spontaneous EPSPs and action potentials in SON neurones (Richard & Bourque, 1992), a response that is sensitive to the application of glutamate receptor antagonists (Bourque & Richard, 1992). These data support the existence of a functional osmosensitive glutamatergic pathway from OVLT to SON in the rat.

How might this circuitry operate *in vivo*? A gradual increase in plasma hyperosmolality is likely to be sensed by OVLT neurones. The activation of an OVLT to SON glutamatergic pathway would provoke an increase in non-NMDA receptor-mediated EPSPs in SON vasopressin-secreting neurones. If sustained, such activation may produce summation of EPSPs and sufficient membrane depolarization to relieve the endogenous Mg^{2+} block of the NMDA receptor–channel complex and the generation of a slow depolarization, and bursting activity. When DAPs are elicited by a burst of action potentials, their summation can trigger the onset of a sustained phasic burst. A schema of the sequence of such events is illustrated in Fig. 12.

In the rat, the response to an osmotic challenge involves both vasopressin and oxytocin-secreting neurones (reviewed in Dyball & Leng, 1989). The lack of a depolarizing OVLT input to oxytocin-secreting SON neurones would suggest either that the osmosensitive input to the oxytocin cells is different from that to the vasopressin neurones, or that this component of the circuit is not involved in osmoreception. Further information is required on the microcircuits that involve oxytocin-secreting cells in osmoreception.

Whether the postsynaptic GABAergic inputs to SON from OVLT participate in osmoregulation remains to be

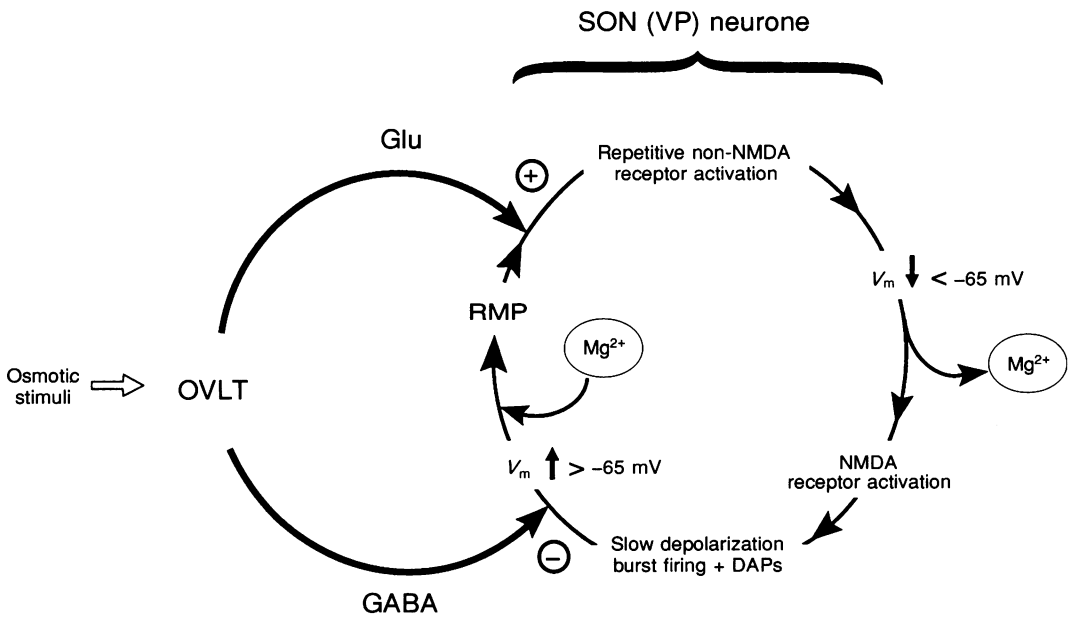

Figure 12. Schematic summary of a proposed mode of operation of the glutamatergic OVLT–SON pathway

Repeated stimulation of the OVLT (e.g. by sustained osmotic stimuli) may activate glutamatergic (Glu) and/or GABAergic OVLT inputs to SON neurones. In the former, repeated activation of non-NMDA glutamate receptors would produce summation of EPSPs, bringing the resting membrane potential (RMP) into a range ($V_m \downarrow \leqslant -65$ mV) that is sufficient to relieve a Mg^{2+} block of the NMDA receptor–channel complex. Slow decay times of the NMDA-mediated EPSPs would be facilitated and contribute to prolonged membrane depolarization, DAPs, bursts of action potentials and phasic firing. Although factors that might activate an OVLT GABAergic input to SON also remain to be defined, the activation of such an input (possibly co-activated by similar stimuli) would have a major 'braking' action on SON vasopressin (VP) cell firing both through provision of a $GABA_A$ receptor-mediated membrane hyperpolarization, and by bringing $V_m \uparrow \geqslant -65$ mV so that the Mg^{2+} blockade of the NMDA receptor–channel complex would resume.

defined. However it is important to note that this input is not selective to vasopressin-secreting neurones. Whatever the source of the stimulus to the OVLT–SON GABAergic pathway, the activation of this component of the OVLT innervation is likely to exert a braking function on the glutamate receptor-mediated (or any other excitatory) input that depolarizes SON neurones.

REFERENCES

ANDREW, R. D. (1987). Endogenous bursting by rat supraoptic neuroendocrine cells is Ca^{2+} dependent. *Journal of Physiology* **384**, 451–465.

ANDREW, R. D. & DUDEK, F. E. (1984). Analysis of intracellularly recorded phasic bursting by mammalian neuroendocrine cells. *Journal of Neurophysiology* **54**, 552–566.

BLACKBURN, R. E., LENG, G. & RUSSELL, J. A. (1987). Control of magnocellular oxytocin neurones by the region anterior and ventral to the third ventricle (AV3V region) in rats. *Journal of Endocrinology* **114**, 253–261.

BOURQUE, C. W. (1986). Calcium-dependent spike after-current induces burst firing in magnocellular neurosecretory cells. *Neuroscience Letters* **70**, 204–209.

BOURQUE, C. W. (1989). Ionic basis for the intrinsic activation of rat supraoptic neurones by hyperosmotic stimuli. *Journal of Physiology* **417**, 263–277.

BOURQUE, C. W. & RICHARD, D. (1992). Glutamatergic excitation of rat supraoptic neurons following osmotic stimulation of the organ vasculosum lamina terminalis (OVLT). *Society for Neuroscience Abstracts* **18**, 481.

CHAUDHRY, M. A., DYBALL, R. E. J., HONDA, K. & WRIGHT, N. C. (1989). The role of interconnection between synaptic nucleus and anterior third ventricular region in osmoregulation in the rat. *Journal of Physiology* **410**, 123–135.

COLLINGRIDGE, G. L., HERRON, C. E. & LESTER, R. A. J. (1988). Frequency-dependent *N*-methyl-D-aspartate receptor-mediated synaptic transmission in rat hippocampus. *Journal of Physiology* **399**, 301–312.

DYBALL, R. E. J. & LENG, G. (1989). Hypothalamic microcircuits involved in osmoregulation. *Biomedical Research* **10**, suppl. 3, 21–32.

ERICKSON, K. R., RONNEKLEIV, O. K. & KELLY, M. J. (1993). Electrophysiology of guinea-pig supraoptic neurones: role of a hyperpolarization-activated cation current in phasic firing. *Journal of Physiology* **460**, 407–425.

GRIBKOFF, V. K. (1991). Electrophysiological evidence for *N*-methyl-D-aspartate excitatory amino acid receptors in the rat supraoptic nucleus in vitro. *Neuroscience Letters* **131**, 260–262.

GRIBKOFF, V. K. & DUDEK, E. (1990). Effects of excitatory amino acid antagonists on synaptic responses of supraoptic neurones in slices of rat hypothalamus. *Journal of Neurophysiology* **63**, 60–71.

HERRON, C. E., LESTER, R. A. J., COAN, E. J. & COLLINGRIDGE, G. L. (1986). Frequency-dependent involvement of NMDA receptors in the hippocampus: a novel synaptic mechanism. *Nature* **322**, 265–268.

HILLE, B. (1984). *Ionic Channels of Excitable Membranes.* Sinauer, Sunderland, MA, USA.

HONDA, K., NEGORO, H., DYBALL, R. E. J., HIGUCHI, T. & TAKANO, S. (1990). The osmoreceptor complex in the rat: evidence for interactions between the supraoptic and other diencephalic nuclei. *Journal of Physiology* **431**, 225–241.

HU, B. & BOURQUE, C. W. (1991). Functional *N*-methyl-D-aspartate and non-*N*-methyl-D-aspartate receptors are expressed by rat supraoptic neurosecretory cells *in vitro*. *Journal of Neuroendocrinology* **3**, 510–514.

JEWELL, P. A. & VERNEY, E. B. (1957). An experimental attempt to determine the site of the neurohypophysis osmoreceptor of the dog. *Philosophical Transactions of the Royal Society* B **240**, 197–324.

JHAMANDAS, J. H., RABY, W., ROGERS, J., BUIJS, R. M. & RENAUD, L. P. (1989). Diagonal band projection towards the hypothalamic supraoptic nucleus: light and electron microscopic observations in the rat. *Journal of Comparative Neurology* **282**, 15–23.

JHAMANDAS, J. H. & RENAUD, L. P. (1986). A γ-aminobutyric-acid-mediated baroreceptor input to supraoptic vasopressin neurones in the rat. *Journal of Physiology* **381**, 595–606.

JOHNSON, A. K. (1985). The periventricular anteroventral third ventricle (AV3V): its relationship with subfornical organ and neural systems involved in maintaining body fluid homeostasis. *Brain Research Bulletin* **15**, 595–601.

KRISCH, B., LEONHARDT, H. & BUCHHEIM, W. (1978). The functional and structural border between the CSF and blood milieu in the circumventricular organs (organum vasculosum laminae terminalis, subfornical organ, area postrema) of the rat. *Cell Tissue Research* **195**, 485–493.

LENG, G., BLACKBURN, R. E., DYBALL, R. E. J. & RUSSELL, J. A. (1989). Role of anterior peri-third ventricular structures in the regulation of supraoptic neuronal activity and neurohypophysial hormone secretion in the rat. *Journal of Neuroendocrinology* **1**, 35–46.

LESTER, R. A. J., QUARUM, M. L., PARKER, J. D., WEBER, E. & JAHR, C. E. (1989). Interaction of 6-cyano-7-nitroquinoxaline-2,3-dione with the *N*-methyl-D-aspartate receptor-associated glycine binding site. *Molecular Pharmacology* **35**, 565–570.

MCALLEN, R. M., PENNINGTON, G. L. & MCKINLEY, M. J. (1990). Osmoresponsive units in sheep median preoptic nucleus. *American Journal of Physiology* **259**, R593–600.

MACDERMOTT, A. B. & DALE, N. (1987). Receptor, ion channels and synaptic potentials underlying the integrative action of excitatory amino acid. *Trends in Neurosciences* **10**, 280–284.

MCKINLEY, M. J., DENTON, D. A., COGHLAN, J. P., HARVEY, R. B., MCDOUGALL, J. G., RUNDGREN, M., SCOGGINS, B. A. & WEISINGER, R. S. (1987). Cerebral osmoregulation of renal Na^+ excretion – a response analogous to thirst and vasopressin release. *Canadian Journal of Physiology and Pharmacology* **65**, 1724–1729.

MCKINLEY, M. J., MCALLEN, R. M., MENDELSOHN, F. A. O., ALLEN, A. M., CHAI, S. Y. & OLDFIELD, B. J. (1990). Circumventricular organs: neuroendocrine interfaces between the brain and the hemal milieu. *Frontiers in Neuroendocrinology* **11**, 91–127.

MAYER, M. L. & WESTBROOK, G. L. (1987). The physiology of excitatory amino acid in the vertebrate central nervous system. *Progress in Neurobiology* **28**, 197–276.

NISSEN, R., BOURQUE, C. W. & RENAUD, L. P. (1993). Membrane properties of organum vasculosum lamina terminalis neurons recorded *in vitro*. *American Journal of Physiology* **264**, R811–815.

PHILLIPS, M. I. & CAMACHO, A. (1987). Neural connections of the organum vasculosum of the lamina terminalis. In *Circumventricular Organs and Body Fluids*, ed. GROSS, P., pp. 157–169. CRC Press, Boca Raton, FL, USA.

RANDLE, J. C. R., BOURQUE, C. W. & RENAUD, L. P. (1986). Characterization of spontaneous and evoked inhibitory postsynaptic potentials in rat supraoptic neurosecretory neurones recorded *in vitro*. *Journal of Neurophysiology* **56**, 1703–1717.

RENAUD, L. P. & BOURQUE, C. W. (1991). Neurophysiology and neuropharmacology of hypothalamic magnocellular neurones secreting vasopressin and oxytocin. *Progress in Neurobiology* **36**, 131–169.

RICHARD, D. & BOURQUE, C. W. (1992). Synaptic activation of rat supraoptic neurones by osmotic stimulation of the organum vasculosum lamina terminalis. *Neuroendocrinology* **55**, 609–611.

ROLAND, B. L. & SAWCHENKO, P. E. (1992). The lamina terminalis is a source of the GABAergic innervation of the magnocellular neurosecretory system. *Society for Neuroscience Abstracts* **18**, 823.

SIBBALD, J. R., HUBBARD, J. E. & SIRRET, N. E. (1988). Responses from osmosensitive neurones of the rat subfornical organ *in vitro*. *Brain Research* **461**, 205–214.

STITT, J. T. (1985). Evidence for the involvement of the organum vasculosum laminae terminalis in the febrile response of rabbits and rats. *Journal of Physiology* **368**, 501–511.

THRASHER, T. N., KEIL, L. C. & RAMSAY, D. J. (1982). Lesions of the organum vasculosum of the lamina terminalis (OVLT) attenuate osmotically-induced drinking and vasopressin secretion in the dog. *Endocrinology* **110**, 1837–1844.

VIVAS, I., CHIARAVIGLIO, E. & CARRER, H. F. (1990). Rat organum vasculosum laminae terminalis in vitro: responses to changes in sodium concentration. *Brain Research* **519**, 294–300.

WILKIN, L. D., MITCHELL, L. D., GANTEN, D. & JOHNSON, A. K. (1989). The supraoptic nucleus: afferents from areas involved in the control of body homeostasis. *Neuroscience* **28**, 573–584.

YANG, C. R., PHILLIPS, M. I. & RENAUD, L. P. (1992). Activation of angiotensin-II type-1 receptor depolarizes neurosecretory neurones of supraoptic nucleus in rat hypothalamic explant. *American Journal of Physiology* **263**, R1333–1338.

YANG, C. R. & RENAUD, L. P. (1991). GABAergic and glutamatergic-mediated synaptic inhibition and excitation in rat supraoptic neurones from activation of organum vaculosum lamina terminalis (OVLT). *Society for Neuroscience Abstracts* **17**, 257.

YANG, C. R., SENATOROV, V. V. & RENAUD, L. P. (1992). NMDA and non-NMDA receptors mediate synaptic activation of supraoptic vasopressin neurons following organum vasculosum lamina terminalis (OVLT) stimulation *in vitro*. *Society for Neuroscience Abstracts* **18**, 676.

Acknowledgements

We thank Drs Bin Hu, Michael Hermes and Ralph Nissen for their constructive criticism of an earlier draft of the manuscript.

Received 16 July 1993; accepted 30 September 1993.